Device design of 1.3μm AlGaInAs-InP narrow strip structure for self-pulsation operation

Guan Hong Wu[*a], Canice G. O'Brien[a], Woon-Ho Seo[b], John F. Donegan[a]
[a] Semiconductor Photonics Group, Physics Department, University of Dublin, Trinity College, Dublin 2, Ireland
[b] Department of Electronic and Electrical Engineering, Sungkyunkwan University, South Korea

ABSTRACT

A complete design of 1.3 μm AlGaInAs/InP narrow stripe semiconductor lasers for self-pulsating operation is realised by using a 2×1D simulation model. This numerical model is based on the effective index method and self-sustained pulsation mechanism in the narrow stripe lasers. The self-pulsation effect is enhanced by the self focusing and defocusing of the optical field which is dependent on the modification of carrier densities in the active region. The resulting AlGaInAs-InP device with compressively strained multi-QWs showed self-pulsation frequency of 3.5 GHz.

Keywords: Self-pulsation, narrow stripe, semiconductor lasers, AlGaInAs, 1.3 μm

1.INTRODUCTION

Optical fiber has minimal dispersion and loss at wavelengths of 1.3 and 1.55 μm, so semiconductor lasers emitting at these wavelengths are important light sources for optical communication systems. Information can be carried through optical fiber by a light wave of varying amplitude (changing brightness). The amplitude is varied by modulating the single-wavelength light coming from a laser source. The laser operates continuous wave (CW) and a modulator is used to convert the output to pulsed format. Due to the high coherence of single wavelength laser source, feedback effects can not be ignored. So an isolator is needed in a transmitter module to eliminate these feedback effects. Inclusion of the modulator and isolator brings the disadvantages of higher cost and bigger size with light sources into optical communication system. Self-pulsation (SP) in semiconductor lasers is a phenomenon which indicates that the emitted optical power varies periodically although the injection currents are kept constant. It has been studied since the diode lasers became available in the 1960's[1]. The first semiconductor lasers exhibited self-pulsation behaviour, although it was designed to operate in CW mode. It was found that high frequency mode beating between longitudinal modes and defects in the active region that act as saturable absorbing areas caused absorptive Q-switching processes. The advances in the technology of material growth and fabrication in subsequent years led to great improvements in material and device quality. The absence of dark-line defects within the laser diode encouraged more research for the explanation of the origins of self-pulsation. It was shown that relaxation oscillation is the underlying mechanism for SP in these devices[2]. Saturable

[*] wugh@tcd.ie; phone 353 1 6082881; fax 353 1 6711759;

Opto-Ireland 2005: Optoelectronics, Photonic Devices, and Optical Networks, edited by
J. G. McInerney, G. Farrell, D. M. Denieffe, L. P. Barry, H. S. Gamble, P. J. Hughes, A. Moore,
Proc. of SPIE Vol. 5825 (SPIE, Bellingham, WA, 2005) · 0277-786X/05/$15 · doi: 10.1117/12.605139

Downloaded from SPIE Digital Library on 04 Feb 2010 to 134.226.1.229. Terms of Use: http://spiedl.org/terms

absorption effects that cause SPs in stripe-geometry lasers have been investigated since 1979[3, 4]. It also causes the SPs in two-section laser diodes[5].

The discovery that SPs could be used to reduce optical feedback noise[6] opened a biggest application area of SP semiconductor lasers, which is in the optical-data storage systems such as CD and DVD devices. The use of quarter wave plate and polarization beam splitter was the traditional way to reduce the amount of feedback noise in these devices. Including these additional components made the whole system less compact in size and more expensive in cost. SP lasers have been also studied for a number of other applications, which include all-optical synchronization, i.e., as optical clocks in all-optical communication systems[7], tunable electrical signal generators[8], all-optical timing extraction[9], tunable optoelectronic bandpass filter[10], etc. Narrow-stripe self-pulsating lasers are usually found in the wavelength region around 800 nm, such as CD and DVD laser diodes. Less common are the two-section distributed feedback (DFB) lasers that operate at communications wavelengths between 1.3 and 1.55 μm. Narrow stripe SP lasers in 1.3 and 1.55 μm are attractive as they will produce laser pulses with very similar characteristics without the need for the modulator. In addition, they are insensitive to optical feedback and so optical isolators are not needed. These will decrease the device size and reduce their costs considerably. They will find potential applications in short-haul or fiber-to-the-home communication systems.

In this paper we present 2×1D simulation models aiming to design a narrow stripe AlGaInAs-InP semiconductor laser structure for SP operation at 1.3 μm. Using AlGaInAs-InP instead of conventional GaInAsP-InP material system is due to the reason that former system has a larger conduction band offset ($\Delta E_c = 0.72\Delta E_g$) at the heterojunctions compared to the smaller conduction band offset ($\Delta E_c = 0.4\Delta E_g$) of the later system. This can reduce carrier leakage from quantum well region thus allowing the device operating at higher temperature[11]. In section II the modified rate equations and some key components related to design a narrow stripe SP laser are discussed. It is shown that the focusing and defocusing of the lateral optical field is crucial to achieving SP in this type of structure. In section III we present the simulated results for AlGaInAs-InP SP laser including detailed device structure parameters. Section IV contains conclusions.

2. SIMULATION MODEL

Some of the earliest attempts to model the dynamics of self-pulsation for narrow stripe semiconductor were based on coupling three rate equations[2]. These describe the evolution of the carrier density within the gain and absorbing layers as two separate sections and the final rate equation described the photon evolution with time. Although these models produced some insight into the mechanisms of self-pulsation they failed to provide any spatial information of the laser diode. As a result of this the self-pulsation mechanism was understood solely in terms of the saturable absorption as a result of the photo-generation of carriers in the absorber section. Later[12] a spatial model was developed in which the diffusion between sections could be treated more rigorously but the optical field was assumed to be stationary throughout the calculation. It was in a subsequent paper[13], that the same author realised that in order to provide a quantitative description of the self-pulsation mechanism both a spatial carrier and optical field time varying model was required and our model is based on this principle.

The schematic diagram of the narrow stripe structure for SP operation is shown in Fig.1. The main features of the laser

Downloaded from SPIE Digital Library on 04 Feb 2010 to 134.226.1.229. Terms of Use: http://spiedl.org/terms

structure are a narrow current stripe, two current blocking layers in the p-doped cladding layer, and a current spreading layer between current blocking layer and active region. The narrow stripe width W < 3μm and the position of the n-doped blocking layer are designed so as to channel the current entering the active layer, so that there is a large variation in current density as one moves from the edge of the stripe region to the region under the current blocking layer. As a result of this, the carrier density profile decreases below its transparency value in the region under the current blocking layer. If the optical field overlaps this region then an absorption region is created. This is one of the prerequisites for obtaining self-pulsation in these types of devices. To ensure that the optical field overlaps these modal absorption regions it is necessary that the index guiding in the lateral direction is weak. Thus through device design the lasing mode will be amplified in the region under the stripe and suffer losses in the region over the current blocking layers. The key parameters that need to be controlled are the amount of current spreading into the regions under the current blocking layers and secondly the width of the optical field and the degree to which it overlaps the absorption regions.

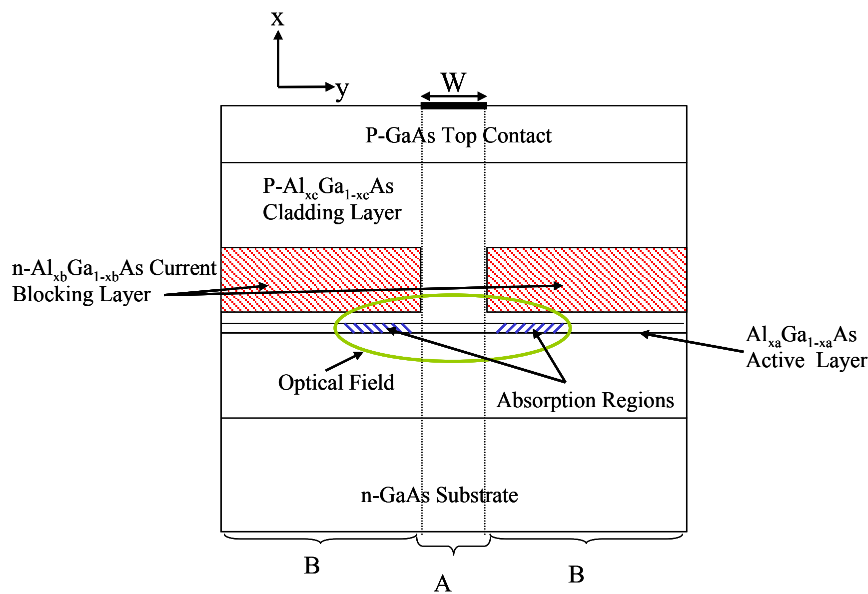

Fig.1 Schematic diagram of narrow stripe self-pulsation laser structure

2.1 Rate Equations

Based on[12] and[13], the variations of the carrier density *N* and photon number *S* are given in form of the following rate equations:

$$\frac{dN(i)}{dt} = \frac{J(i)}{qd_a} - R_{sp}(i) - \frac{N(i)}{\tau_{nr}} + D_a \frac{\left(N(i-1) - 2N(i) + N(i+1)\right)}{\Delta^2} - \frac{c}{n_g}\frac{g(i)\Gamma(i)S}{V_a} \tag{2.1}$$

Downloaded from SPIE Digital Library on 04 Feb 2010 to 134.226.1.229. Terms of Use: http://spiedl.org/terms

$$\frac{dS}{dt} = \frac{c}{n_g}(G - G_{th})S + \beta V_a \iint_{Total} R_{sp} |\phi|^2 \, dxdy \qquad (2.2)$$

The active region is divided into sections with constant carrier density $N(i)$. These carrier densities between neighbouring sections are coupled through the ambipolar diffusion term D_a, which describes the electron and hole drift and diffusion effects collectively. They are also coupled through the stimulated emission term (final term on the right hand side in (2.1)). n_g is the group refractive index and Γ is the confinement factor. In (2.2), β denotes the spontaneous emission factor that describes the fraction of spontaneous emission coupled into the lasing mode.

If the active region is divided into n sections, the solution of equation (2.1) and (2.2) requires the solution of $n+1$ ordinary differential equations. Since these equations are coupled, it is important when considering numerical methods of solution to consider that the error introduced in incrementing each equation over a time step d_t, must be calculated for each equation and the time step should be adjusted to meet the specific fractional error applied by the worst case. Other considerations, such as, the safeguarding against the accumulation in global errors is described further in[18]. The numerical scheme that has been used to meet the requirements is the fourth order Runge-Kutta driver with adaptive stepsize control.

2.2 Self-Pulsation by Simulation

In order to use the effective index method effectively, the waveguide can be broken into two sections. Section A is the pumped epitaxial layer region under the current stripe and section B is the epitaxial layer region under the blocking layers (see Fig.1). For each of the n lateral sections, the one-dimensional wave equation is solved in the transverse direction. An equivalent one-dimensional waveguide is then formed in the lateral direction from the effective propagation constants. Since the current blocking layer has a lower refractive index than that of the cladding, an effective index step is formed in the lateral direction. This index step is very important to ensure that sufficient confinement of the lateral optical field to avoid overlapping the absorption regions in the active layer at early stage of the pulsation process. The gain and refractive index are changed with carrier density through the linewidth enhancement factor α. So the effective index step between A and B sections changes with the carrier density too. The reduction in refractive index with increasing carrier density has the effect of reducing the transverse electric field confinement and at the same time causing a reduction in the effective index. In order to ensure that the 2×1D effective index simulation is as efficient as possible, instead of solving the one dimensional wave equation for the effective index and transverse confinement factor and subsequently solving the lateral effective slab waveguide each time, the two dimensional field needs to be calculated. A database was set up so that for a given carrier density the effective index and transverse confinement factor can be interpolated without the need to calculate these for each of the n sections.

The AlGaAs-GaAs material system was choosen to simulate because of its stable SP operation. The layer structure is shown in Fig.1. Changing the Aluminium mole fraction xb in blocking layer can vary the effective index step between

Downloaded from SPIE Digital Library on 04 Feb 2010 to 134.226.1.229. Terms of Use: http://spiedl.org/terms

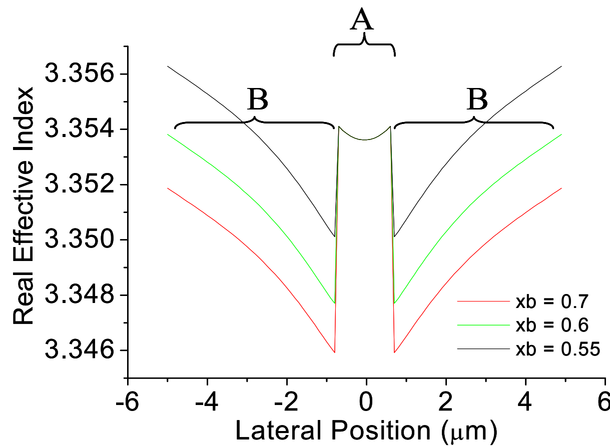

Fig.2 Variation in the effective index steps in the lateral direction with different Al mole fraction in blocking layer.

the A and B sections. The greatest reduction in effective index occurs where the carrier density is highest, under the current stripe. As the carrier density decreases moving laterally to either side of the current stripe, the reduction in the effective index becomes less. These factors combine to create the effective profiles seen in Fig.2. The simulated SP results are illustrated in Fig.3 and Fig.4. The SP frequency is 1.45 GHz and bias current is 30mA. From Fig.3 (b), we see that as the carrier density reaches its peak the pulse begins to form and as the output power increases the carrier density reduces due to stimulated emission.

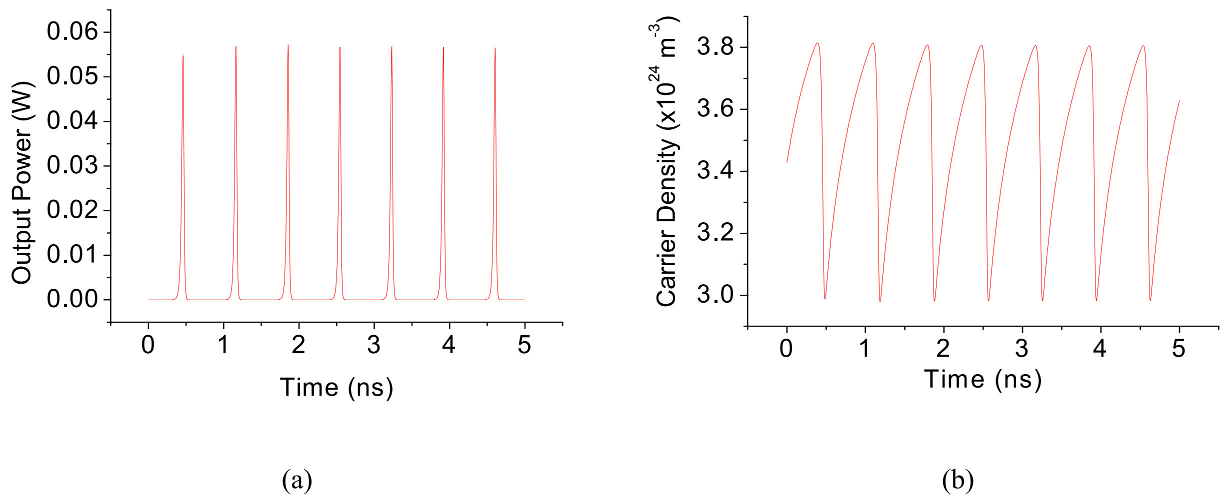

(a) (b)

Fig.3 The output power evolution with time (a) shows self-pulsation behaviour and corresponding carrier density variation within the central section of active region (b).

Downloaded from SPIE Digital Library on 04 Feb 2010 to 134.226.1.229. Terms of Use: http://spiedl.org/terms

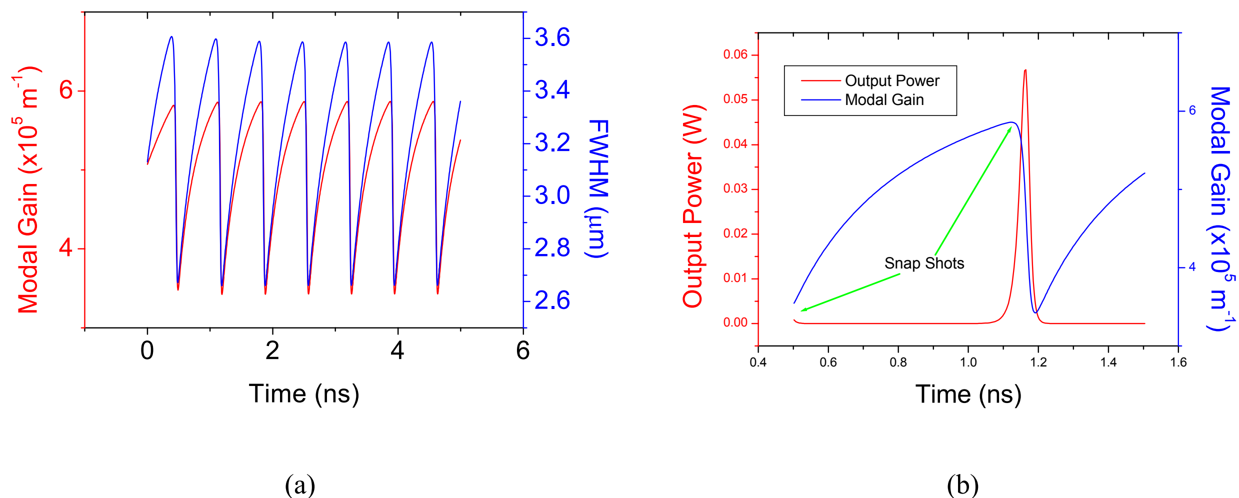

(a) (b)

Fig.4 (a) The FWHM of the lateral optical field is synchronized with modal gain. (b) The emission of a pulse over 1 ns timescale.

An important feature of this type of self pulsation is that the increase in carrier density before a pulse is emitted reduces the effective index step in the lateral direction and as a result the full width half maximum (FWHM) of the lateral field increases mirroring the behaviour of the modal gain as seen in Fig.4 (a). With the resultant emission of the pulse and rapid decrease in the carrier density the effective index again increases in the central section resulting in a focusing of the lateral field and a decrease in the FWHM. In order to gain further insight into the cause of the self-sustained modulation, we concentrate on the spatial distribution of key parameters over the lifetime of a single pulse. Although the pulse itself occurs over of a time interval of the order of 100ps the build up of the modal gain profile is much slower. For this reason we have examined the pulse behaviour over 1ns from 0.5ns to 1.5ns as seen in Fig.4 (b). It can be seen that the carrier density profile is at a maximum in the region under the stripe at 1.1ns just at the beginning of the pulse emission. The 0.5ns profile indicates that after pulse emission, the carrier density is now depleted in the central region due to stimulated emission. But in the side regions it has increased and this can be explained due to the photo-generation of carriers in the absorber section. As the pulse is formed the optical field extends into the absorption regions, where photons are absorbed resulting in an increase in carrier density in these regions. This photo generated increase in the carrier density reduces the amount of absorption within these regions, the absorption therefore begins to saturate. This process is aided by the self-focusing of the optical field due to the increase in refractive index under the stripe as the carrier density is reduced due to stimulated emission. The self-focusing and defocusing of the optical field enhances and sustains the SP. These simulation results for AlGaAs-GaAs narrow stripe lasers were verified well by the experimental results from the same device[19]. This illustrates that our 2×1D model is successful.

3. Design a Narrow Stripe AlGaInAs-InP Self-Pulsation Laser

When moving from AlGaAs-GaAs at 780 nm to AlGaInAs-InP material system at 1.3 and 1.55 μm, the effects of Auger recombination and inter-valance band absorption (IVBA) on the SP behaviour need to be considered now. Unlike the GaAs substrate, InP has a wider bandgap than the active region and therefore has the advantage that none of the lasing light is absorbed within the substrate. It is also an ideal material to be used in the blocking layer since it has the highest

Downloaded from SPIE Digital Library on 04 Feb 2010 to 134.226.1.229. Terms of Use: http://spiedl.org/terms

refractive index difference to that of the active region so that one can vary the cladding layer index while ensuring that the optical field will be confined sufficiently at the same time. Due to the reason that the differential gain is increased[20], and there is a reduction in the Auger coefficient and inter-valence band absorption for quantum well structures[21], we use QW structure in the active region. A single QW offers a large differential gain and the low transparency carrier density which results to a low nonradiative recombination loss due to the cubic term of Auger loss, $C_{auger}N^3$. But very little optical confinement makes the modal gain insufficient to overcome the total losses in the laser. With increasing the QW number, the optical field can be confined more in active region. But the transparency carrier density increases as well so the nonradiative recombination losses increase. There is a compromise on choosing suitable QW numbers. In our structure, 6 QWs are to be used in the active region as the nonradiative recombination current in AlGaInAs lasers is smaller than the non-radiative recombination current in InGaAsP structure at room temperature[11]. According to previous work the Auger coefficient is chosen to be 3.5×10^{-30} cm^6s^{-1} [22] and IVBA coefficient is estimated at a value of 8.2×10^{-21} m^2 for our structure[23]. The device length is 250 μm and pump threshold current is 28 mA. We use n-InP as blocking layer material. Its refractive index can be changed by modifying the doping level[24]. This is one of novel features in our structure design. The simulated device structure parameters that lead to SP operation are listed in Table 1.

Table 1 List of the layers of the laser structure

Layer	Composition	Thickness (μm)	Refractive index
n-substrate	InP	0.5	3.1987
n-cladding	InP	1.5	3.207
SCH	AlGaInAs	0.035	3.363
QW	$Al_{0.28}GaIn_{0.53}As$	0.006	3.530(3.515-3.540)
barrier	$Al_{0.59}GaIn_{0.53}As$	0.01	3.363(3.355-3.373)
QW	$Al_{0.28}GaIn_{0.53}As$	0.006	3.530(3.515-3.540)
barrier	$Al_{0.59}GaIn_{0.53}As$	0.01	3.363(3.355-3.373)
QW	$Al_{0.28}GaIn_{0.53}As$	0.006	3.530(3.515-3.540)
barrier	$Al_{0.59}GaIn_{0.53}As$	0.01	3.363(3.355-3.373)
QW	$Al_{0.28}GaIn_{0.53}As$	0.006	3.530(3.515-3.540)
barrier	$Al_{0.59}GaIn_{0.53}As$	0.01	3.363(3.355-3.373)
QW	$Al_{0.28}GaIn_{0.53}As$	0.006	3.530(3.515-3.540)
barrier	$Al_{0.59}GaIn_{0.53}As$	0.01	3.363(3.355-3.373)
QW	$Al_{0.28}GaIn_{0.53}As$	0.006	3.530(3.515-3.540)
SCH	AlGaInAs	0.035	3.363
Current spreading	p-InP	0.15	3.207
Blocking	n-InP	1.0	3.1670(3.130-3.180)
p-cladding	InP	1.0	3.207
p-contact	$Ga_{0.47}In_{0.53}As$	0.2	3.207(3.155-3.480)

* In section A there is no current spreading layer. The total p-cladding layer thickness is 2 μm.

Downloaded from SPIE Digital Library on 04 Feb 2010 to 134.226.1.229. Terms of Use: http://spiedl.org/terms

Similar to the simulation of the AlGaAs device in last section, some plots are shown as follows. Fig.5 shows the obtained SP behavuour under the pump current of 35 mA which is equal to $1.2I_{th}$. The SP frequency is 3.5 GHz and increases with increasing the pump currents. Our structure can exhibit SP operation up to a pump current of 55 mA.

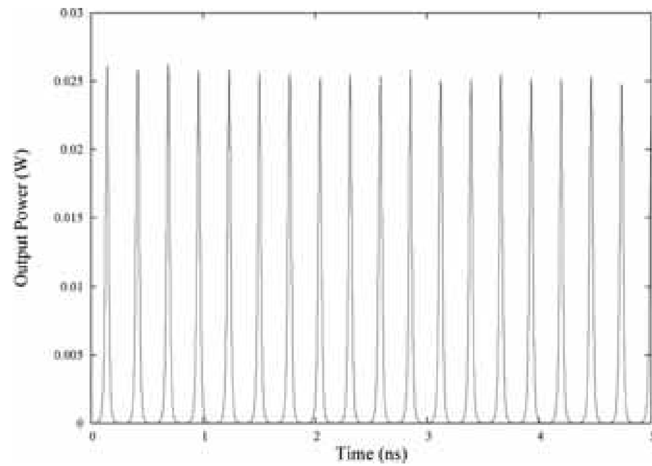

Fig.5 The SP spectrum from our design under the pump current of 35 mA ($1.2I_{th}$).

The pulse behaviour over 0.25 ns from 0.2 ns to 0.45 ns is shown in Fig.6. Compare to Fig.4 (b) the modal gain profile builds up much quicker in this material system. This is due to the higher carrier mobility with lower electron effective mass in AlGaInAs material[25]. Similar self-focusing and defocusing effects in the FWHM of lateral field is illustrated in Fig.7.

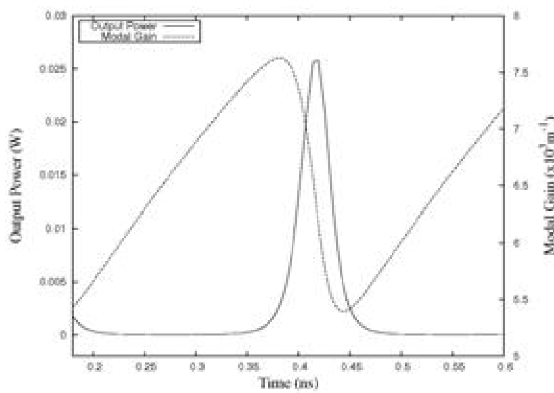

Fig.6 The emission of a pulse over 0.25 ns timescale.

Downloaded from SPIE Digital Library on 04 Feb 2010 to 134.226.1.229. Terms of Use: http://spiedl.org/terms

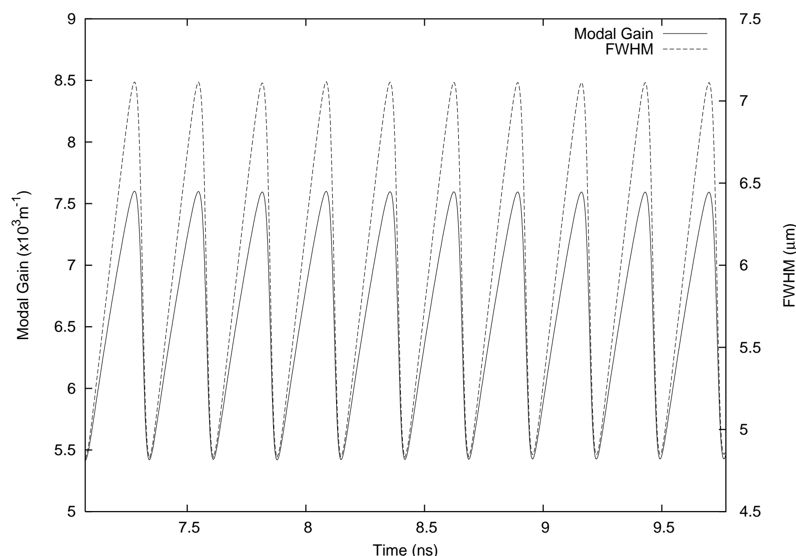

Fig.7 The FWHM of the lateral optical field is synchronized with modal gain.

4. CONCLUSIONS

A 2×1D model that based on effective index method has been developed to simulate the carrier density dependent spatial and temporal variations of the SP laser waveguide and their effects on the SP behaviour. The use of the effective index method was an important first step, in that it allowed one to identify the degree to which the structure was weakly guided. It also provided a criterion for measurement of the lateral effective index step and the variation of the refractive index of the blocking layer material. Within the effective refractive index framework it was possible through the calculation of the full width half maximum (FWHM) of the lateral field, to show that the self-focusing and defocusing of the FWHM was crucial to achieving self-pulsation from the model in this type of structure. Based on the successful simulation of AlGaAs-GaAs SP lasers, a narrow stripe laser structure in AlGaInAs-InP material system at 1.3 μm for SP operation was also designed. It showed higher frequency of SP and lower threshold current. Our design uses InP as blocking layer material which has better thermal conductivity and is easy to grow. Its refractive index can be controlled through changing doping level in the current blocking layer.

REFERENCES

1. N. G. Basov, "Dynamics of Injection Lasers", *IEEE J. Quantum Electron.*, **QE-4**, pp.855-867, 1968.
2. M. Yamada, "A Theoretical Analysis of Self-Sustained Pulsation Phenomena in Narrow-Stripe Semiconductor Lasers", *IEEE J. Quantum Electron.*, **29**, pp.1330-1336, 1993.
3. T. L. Paoli, "Saturable Absorption Effects in the Self-Pulsating (AlGa)As Junction Lasers", Appl. Phys. Lett., Vol.**34**, pp.652-655, 1979.
4. M. Ueno and R. Lang, "Conditions for Self-Sustained Pulsation and Bistability in Semiconductor Lasers", *J. Appl. Phys.*, **58**, pp.1689-1692, 1985.

Downloaded from SPIE Digital Library on 04 Feb 2010 to 134.226.1.229. Terms of Use: http://spiedl.org/terms

5. E. A. Avrutin, "Analysis of Spontaneous Emission and Noise in Self-Pulsating Laser Diodes", *Proc. Inst. Elect. Eng.*, **140**, pp.16-20, 1993.

6. S. Matsui, H. Takiguchi, H. Hayashi, S. Yamamoto, S. Yano, and T. Hijikata, "Suppression of Feedback Induced Noise in Short V-Channel Substrate Inner-stripe Lasers with Self-oscillations", *Appl. Phys. Lett.*, **43**, pp.219-221, 1983.

7. P. Phelan, G. Farrel, and J. Hegarty, "All-optical Synchronization and Frequency Division of Mode-locked Pulse", *IEEE Photon. Technol. Lett.*, **4**, pp.930-932, 1992.

8. Y. Simler, J. Gamelin, and S. Wang, "Pulsation Stabilization and Enhancement in Self-pulsating Laser Diodes", *IEEE Photon. Technol. Lett.*, **4**, pp.329-332, 1992.

9. P. E. Barnsley and H. J. Wickes, "All-optical clock recovery from 5 Gb/s RZ data using a self-pulsating 1.56 μm laser diode", *IEEE Photon. Technol. Lett.*, **3**, pp.942-945, 1991.

10. S. E. M. Dundley, J. M. Guzman, T. Quinlan, and S. D. Walker, "Tunable Optoelectronics Bandpass filtering using a Simple Self-pulsating Two-section Lasers", *Optics Express*, **11**, pp.151-157, 2003.

11. T. Higashi, S. J. Sweeney, A. F. Philips, A. R. Adams, E. P. O'Reilly, T. Uchida, and T. Fuji, "Observation of reduced nonradiative current in 1.3-μm AlGaInAs-InP strained MQW lasers", *IEEE Photon. Technol. Lett.*, **11**, pp.409-411, 1999.

12. T. Takayama, O. Imafuji, H. Sugiura, M. Yuri, H. Naito, M. Kume and K. Itoh, "Low-noise and high-power GaAlAs laser diodes with a new real refractive index guided structure.", *Jpn. J. Appl. Phys.*, **34**, pp.3533-3542, 1995.

13. M. Yuri, J. S. Harris, T. Takayama, O. Imafuji, H. Naito, M. Kume, K. Itoh and T. Baba, "Two-dimensional analysis of self-sustained pulsation for narrow-stripe AlGaAs lasers", *IEEE J. Select. Topics. Quantum Electron.*, **1**, pp.473-479, 1995.

14. H. Yonezu, I. Sakuma, K. Kobayashi, T. Kamejima, M. Ueno and Y. Nannichi, "GaAs-$Al_xGa_{1-x}As$ double heterostructure planar stripe laser", *Japan J. Appl. Phys.*, **12**, pp.1585-1592, 1973.

15. G. Lengyel, P. Meissner, E. Patzak, and K. H. Zschauer, "An analytical solution of the lateral current spreading and diffusion problem in narrow oxide stripe (GaAl)As/GaAs DH laser", *IEEE J. Quantum Electron.*, **18**, pp.618-625, 1982.

16. R. Papannareddy, W. E. Ferguson, J. K. Butler, "Four models of lateral current spreading in double-heterostructure stripe-geometry lasers", *IEEE J. Quantum Electron.*, **24**, pp.60-65, 1988.

17. W. B. Joyce, R. W. Dixon, "Electrical characteristization of heterostructure laser", *J. Appl. Phys.*, **49**, pp.3719-3728, 1978.

18. W. H. Press, B. P. Flannery, S. A. Teukolsky, W. T. Vetterling, "Numerical Recipes in C", *Cambridge University Press*, 1988.

19. S. A. Lynch, "Pulse formation and dynamics in self-pulsating semiconductor laser diodes", *PhD Thesis*, University of Dublin, Trinity College, 1999.

20. P. Zory, "Quantum Well Lasers", *Academic Press*, 1993.

21. Y. Zou, J. Osinski, P. Grodzinski, P. Dapkus, W. Rideout, W. Sharfin, and F. Crawford, "Effect of Auger recombination and differential gain on the temperature sensitivity of 1.5 μm quantum well lasers", *Appl. Phys. Lett.*, **62**, pp.175-177, 1993.

22. S. R. Selmic, T. M. Chou, J. Sih, J. B. Kirk, A. Mantie, J. K. Butler, D. Bour, and G. A. Evans, "Design and characterization of 1.3 μm AlGaInAs-InP multiple-quantum-well lasers", *IEEE J. Sel. Top. Quantum Electron.*, **7**, pp.340-349, 2001.

23. J. Taylor and V. Tolstikhin, "Intervalence band absorption in InP and related materials for optoelectronic device modeling", *J. Appl. Phys.*, **87**, pp.1054-1059, 2000.

Downloaded from SPIE Digital Library on 04 Feb 2010 to 134.226.1.229. Terms of Use: http://spiedl.org/terms

24. L. Chusseau, P. Martin, C. Brasseur, C. Alibert, P. Herve, P. Arguel, F. L. Dupuy, and E. V. K. Rao, “Carrier-induced change due to doping in refractive index of InP: measurement at 1.3 and 1.5 μm”, *Appl. Phys. Lett.*, **69**, pp.3054-3056, 1996.
25. J. C. L. Yong, J. Rorison, and I. H. White, “1.3 μm quantum-well InGaAsP, AlGaInAs, and InGaAsN laser material gain: A theoretical study”, *IEEE J. Quantum Electron.*, **38**, pp.1553-1564, 2002.

Downloaded from SPIE Digital Library on 04 Feb 2010 to 134.226.1.229. Terms of Use: http://spiedl.org/terms